Supplementary Material
DeepCA: Deep Learning-based 3D Coronary Artery Tree Reconstruction from Two 2D Non-simultaneous X-ray Angiography Projections

Yiying Wang[1] Abhirup Banerjee[1,2] Robin P. Choudhury[2] Vicente Grau[1]
[1]Institute of Biomedical Engineering, Department of Engineering Science, University of Oxford, UK
[2]Division of Cardiovascular Medicine, Radcliffe Department of Medicine, University of Oxford, UK

1. Appendix

We show additional qualitative results for our proposed DeepCA model, 4 baseline models, and 3 ablation models. All the 3D reconstructions on the CCTA test dataset and real clinical ICA dataset are binarised with a threshold of 0.5 before evaluation, reprojection, and visualisation. All the 2D reprojections are binarised with a threshold of 0 before evaluation and visualisation.

Four baseline models: We replace the 3D U-Net in WCGAN-GP with Unet++ [4] (termed as Un2+), with Unet+++ [1] (termed as Un3+), and with DSConv Net [2] (termed as DSCN). We also implement the 3D convolutional vision transformer GAN [3] (termed as CVTG).

Three ablation models: (1) WCGAN-GP (termed as WGP), (2) WCGAN-GP + latent CTLs (termed as +CTLs), and (3) WCGAN-GP + DSConv critic (termed as +DSCC).

1.1. Projection Geometry

In the generation of simulated projections on the CCTA dataset, we use the projection geometry of real coronary angiography to simulate the two cone-beam forward projections, the parameters of which are illustrated in Table 1. In order to simulate breathing and cardiac motions on the second projection plane, we rotate the CCTA data randomly for both primary and secondary angles ranging from -10° to 10° and add translations of -8 mm to 8 mm in both horizontal and vertical directions.

1.2. Qualitative Results on 3D CCTA Test Dataset

We present 5 CCTA test data samples for qualitative analysis. Before evaluation, we rigidly register the ground truth (original CCTA test data) to the 3D reconstruction. Figure 1 shows the original ground truth and the 3D reconstructions generated by all the models visualised from the front view. Figure 2 illustrates the corresponding voxel-wise prediction errors in terms of Chamfer ℓ_2 distance (CD(ℓ_2)) between the ground truth and the 3D reconstruction.

1.3. Qualitative Results on 2D Clinical ICA Dataset

We present the 3D reconstructions by all the models and the corresponding 2D reprojections when testing on the out-of-distribution 2D real clinical ICA dataset of 8 patients. Figure 3 displays the 3D reconstructions by all the models. Figure 4 illustrates the comparisons on the first projection plane between the original ICA data and the reprojections. Before evaluation on the second and additional projection planes, we first rigidly register the original ICA data to the reprojections. Figures 5 and 6 present the comparisons on the second and additional projection planes between the registered ICA data and the reprojections.

1.4. Discussion

We can see from Figs. 1 and 2 that our proposed DeepCA model has successfully reconstructed all the branches and maintained the vessel connectivity, while for the baseline models, there are many missing and/or broken branches visible. Although there is no corresponding 3D ground truth for the real clinical ICA data, we observe the same results in Fig. 3. In particular, some 3D reconstruction results on clinical ICA data from the baseline models miss the vascular features almost entirely, such as the reconstructions by model Un2+ and Un3+ on patients 2, 3, and 8.

The qualitative evaluation results on all three projection planes, as illustrated in Figs. 4 to 6, demonstrate the superiority of our proposed DeepCA model's performance on real clinical ICA data as well. These results indicate that our proposed DeepCA model has the best performance in vessel topology preservation and recovery of missing features.

Moreover, in all the qualitative results from the 3 ablation models, we can find that each component of our proposed DeepCA model has contributed to the final reconstruction performance with more vascular features recovered and broken branches connected.

Table 1. The projection geometry to simulate cone-beam forward projections on the CCTA dataset, in order to resemble the real ICA settings. The CCTA data with motion is used on the second projection plane to simulate the breathing and cardiac motions; here we rotate the CCTA data randomly for both primary and secondary angles ranging from -10° to 10° and add translations of -8 mm to 8 mm in both horizontal and vertical directions.

	First Projection Plane	Second Projection Plane
Phantom	Original 3D CCTA Data	3D CCTA Data with Motion
Detector Spacing	$0.2769 \times 0.2769\ mm^2$ to $0.2789 \times 0.2789\ mm^2$	
Detector Size	512×512	
Volume Spacing	$90 \times 90 \times 90\ mm^3$ to $105 \times 105 \times 105\ mm^3$	
Volume Size	$128 \times 128 \times 128$	
Distance for Source to Detector (DSD)	970 mm to 1010 mm	1050 mm to 1070 mm
Distance for Source to Origin (DSO)	745 mm to 785 mm	$\pm$ 3 mm to the First Projection
Primary Angle	18° to 42°	$-8°$ to 8°
Secondary Angle	$-8°$ to 8°	18° to 42°

References

[1] Huimin Huang, Lanfen Lin, Ruofeng Tong, Hongjie Hu, Qiaowei Zhang, Yutaro Iwamoto, Xianhua Han, Yen-Wei Chen, and Jian Wu. Unet 3+: A full-scale connected unet for medical image segmentation. In *ICASSP 2020-2020 IEEE International Conference on Acoustics, Speech and Signal Processing (ICASSP)*, pages 1055–1059. IEEE, 2020. 1

[2] Yaolei Qi, Yuting He, Xiaoming Qi, Yuan Zhang, and Guanyu Yang. Dynamic snake convolution based on topological geometric constraints for tubular structure segmentation. In *Proceedings of the IEEE/CVF International Conference on Computer Vision (ICCV)*, pages 6070–6079, October 2023. 1

[3] Pinxian Zeng, Luping Zhou, Chen Zu, Xinyi Zeng, Zhengyang Jiao, Xi Wu, Jiliu Zhou, Dinggang Shen, and Yan Wang. 3D CVT-GAN: A 3D convolutional vision transformer-GAN for PET reconstruction. In *Medical Image Computing and Computer Assisted Intervention – MICCAI 2022*, pages 516–526, 2022. 1

[4] Zongwei Zhou, Md Mahfuzur Rahman Siddiquee, Nima Tajbakhsh, and Jianming Liang. UNet++: A nested U-Net architecture for medical image segmentation. In *Deep Learning in Medical Image Analysis and Multimodal Learning for Clinical Decision Support*, pages 3–11, 2018. 1

Figure 1. 3D reconstruction results on 5 CCTA test data from all the models. From left to right: 5 CCTA test data samples. Row 1: The 3D ground truth. From row 2 to the end: The 3D reconstruction results by our proposed DeepCA model, WGP, +CTLs, +DSCC, Un2+, Un3+, DSCN, and CVTG.

Figure 2. The corresponding voxel-wise prediction errors in terms of CD(ℓ_2) between the ground truth and 3D reconstruction, after rigidly registering the ground truth to the reconstructions from all the models. From left to right: 5 CCTA test data samples. From top to bottom: the prediction errors by our proposed DeepCA model, WGP, +CTLs, +DSCC, Un2+, Un3+, DSCN, and CVTG.

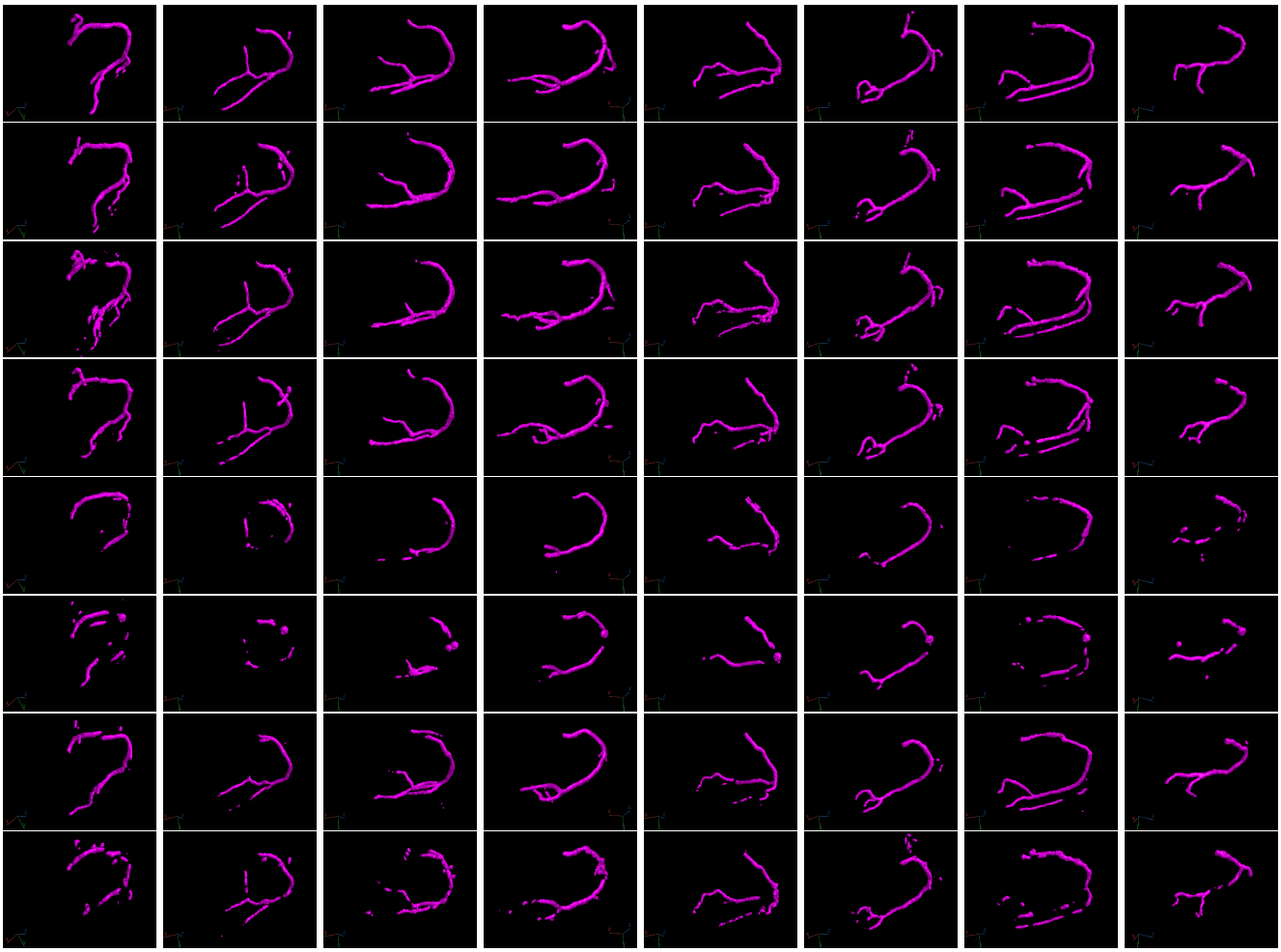

Figure 3. 3D reconstruction results of 8 real clinical ICA data from all the models. From left to right: 8 patients. From top to bottom: 3D reconstruction results by our proposed DeepCA model, WGP, +CTLs, +DSCC, Un2+, Un3+, DSCN, and CVTG.

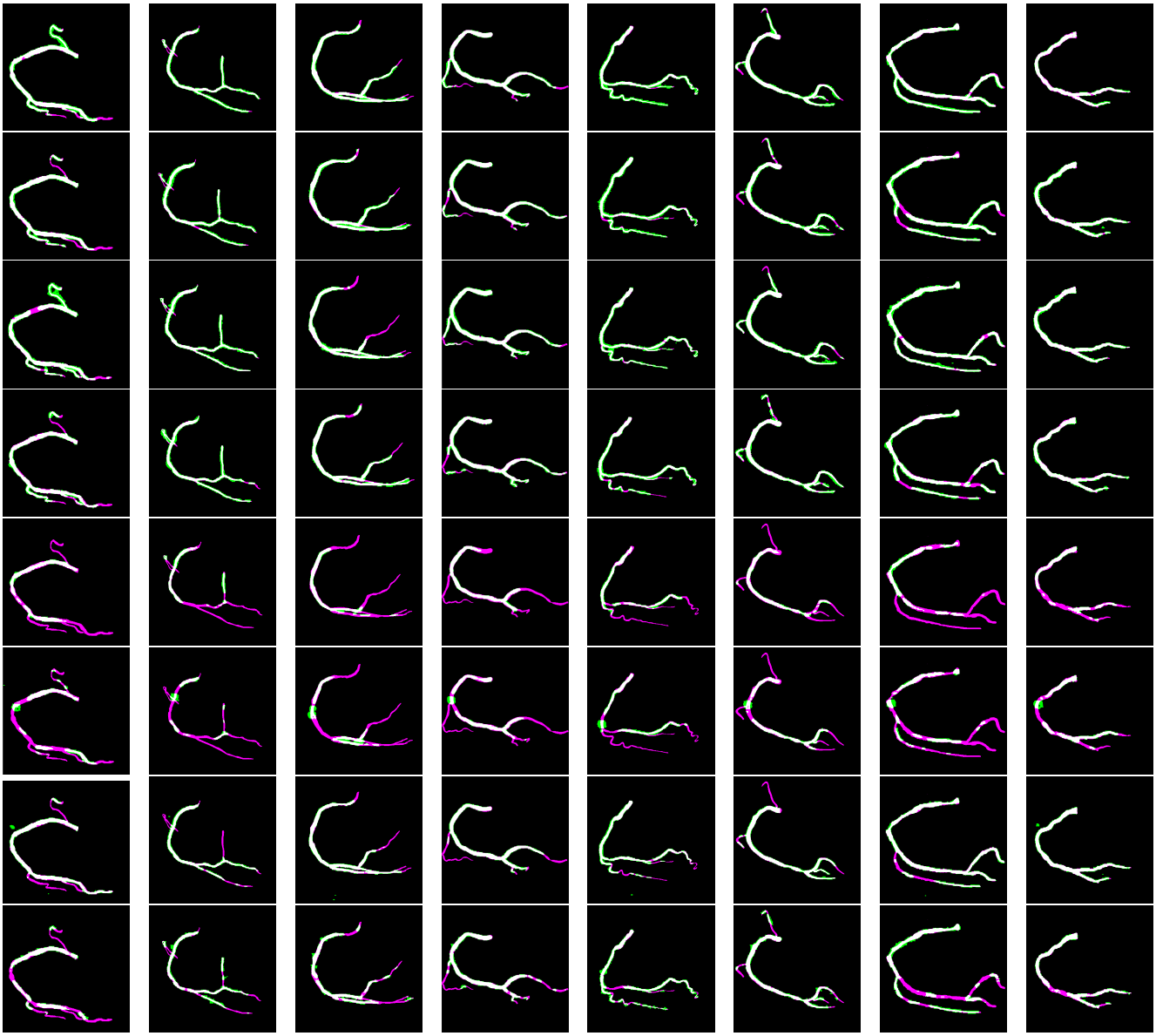

Figure 4. The comparisons on the first projection plane between the original clinical ICA data and the reprojections of the 3D reconstructions generated from all the models. From left to right: 8 patients. From top to bottom: comparisons between the original ICA data and the reprojections from the reconstructions by our proposed DeepCA model, WGP, +CTLs, +DSCC, Un2+, Un3+, DSCN, and CVTG. Colour purple presents original ICA data, green is reprojection, and white shows the overlap.

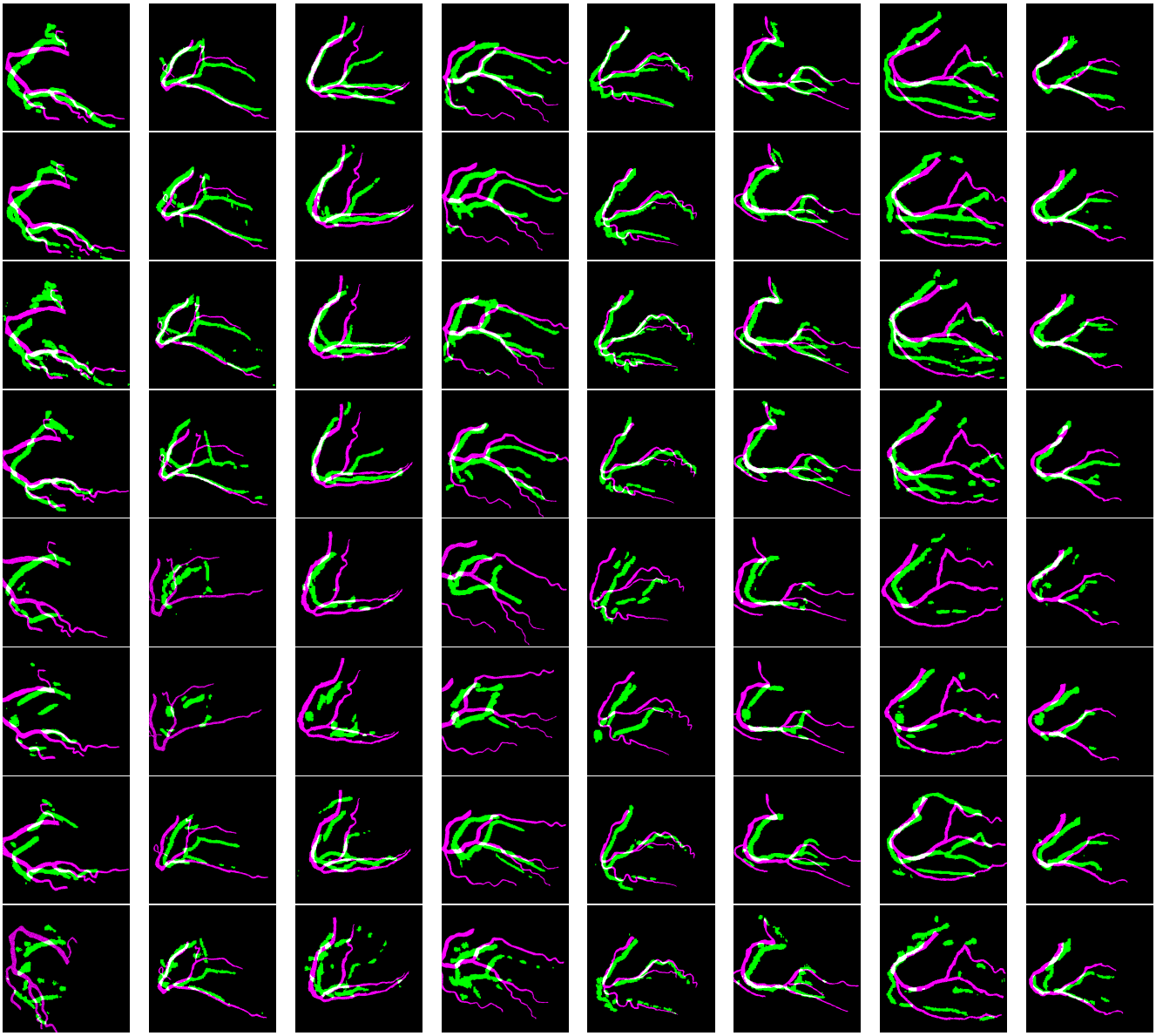

Figure 5. The comparisons on the second projection plane between the registered ICA data and the reprojections of the 3D reconstructions generated from all the models. The ICA data (in purple) are rigidly registered to the reprojections (in green) before comparison. From left to right: 8 patients. From top to bottom: comparisons between the registered ICA data and the reprojections from the reconstructions by our proposed DeepCA model, WGP, +CTLs, +DSCC, Un2+, Un3+, DSCN, and CVTG. Colour purple presents registered ICA data, green is reprojection, and white shows the overlap.

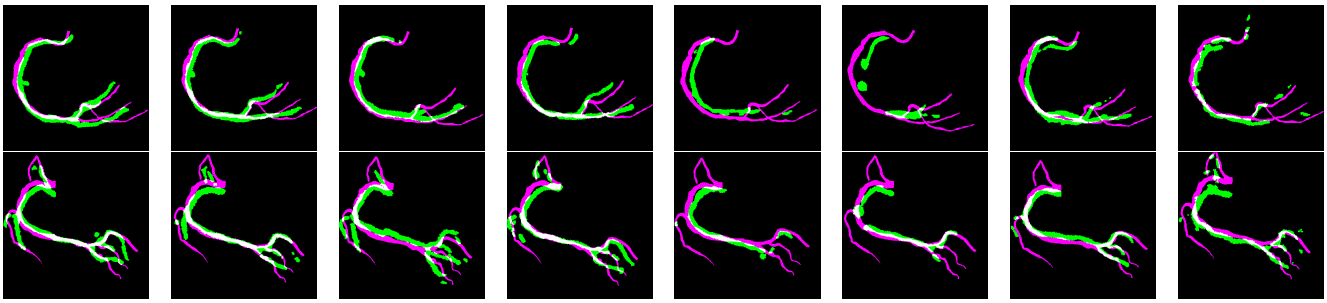

Figure 6. The comparisons on the additional (third) projection plane between the registered ICA data and the reprojections of the 3D reconstructions generated from all the models. The ICA data (in purple) are rigidly registered to the reprojections (in green) before comparison. From top to bottom: 2 patients who have additional ICA projections. From left to right: comparisons between the registered ICA data and the reprojections from the reconstructions by our proposed DeepCA model, WGP, +CTLs, +DSCC, Un2+, Un3+, DSCN, and CVTG. Colour purple presents registered ICA data, green is reprojection, and white shows the overlap.